⌘ *Author's Choice*

THE JOURNAL OF BIOLOGICAL CHEMISTRY VOL. 285, NO. 52, pp. 40771–40776, December 24, 2010

Arginine 104 Is a Key Catalytic Residue in Leukotriene C_4 Synthase*

Received for publication, February 9, 2010, and in revised form, September 28, 2010 Published, JBC Papers in Press, October 27, 2010, DOI 10.1074/jbc.M110.105940

Agnes Rinaldo-Matthis[‡], Anders Wetterholm[‡], Daniel Martinez Molina[§], Johanna Holm[‡], Damian Niegowski[‡], Eva Ohlson[‡], Pär Nordlund[§], Ralf Morgenstern[¶], and Jesper Z. Haeggström[‡1]

From the Divisions of [‡]Chemistry 2 and [§]Biophysics, Department of Medical Biochemistry and Biophysics, and [¶]Institute of Environmental Medicine, Karolinska Institutet, S-171 77 Stockholm, Sweden

Human leukotriene C_4 synthase ($hLTC_4S$) is an integral membrane enzyme that conjugates leukotriene (LT) A_4 with glutathione to form LTC_4, a precursor to the cysteinyl leukotrienes (LTC_4, LTD_4, and LTE_4) that are involved in the pathogenesis of human bronchial asthma. From the crystal structure of $hLTC_4S$, Arg-104 and Arg-31 have been implicated in the conjugation reaction. Here, we used site-directed mutagenesis, UV spectroscopy, and x-ray crystallography to examine the catalytic role of Arg-104 and Arg-31. Exchange of Arg-104 with Ala, Ser, Thr, or Lys abolished 94.3–99.9% of the specific activity against LTA_4. Steady-state kinetics of R104A and R104S revealed that the K_m for GSH was not significantly affected. UV difference spectra of the binary enzyme-GSH complex indicated that GSH ionization depends on the presence of Arg-104 because no thiolate signal, with λ_{max} at 239 nm, could be detected using R104A or R104S $hLTC_4S$. Apparently, the interaction of Arg-104 with the thiol group of GSH reduces its pK_a to allow formation of a thiolate anion and subsequent nucleophilic attack at C6 of LTA_4. On the other hand, exchange of Arg-31 with Ala or Glu reduced the catalytic activity of $hLTC_4S$ by 88 and 70%, respectively, without significantly affecting the k_{cat}/K_m values for GSH, and a crystal structure of R31Q $hLTC_4S$ (2.1 Å) revealed a Gln-31 side chain pointing away from the active site. We conclude that Arg-104 plays a critical role in the catalytic mechanism of $hLTC_4S$, whereas a functional role of Arg-31 seems more elusive. Because Arg-104 is a conserved residue, our results pertain to other homologous membrane proteins and represent a structure-function paradigm probably common to all microsomal GSH transferases.

Human leukotriene C_4 synthase ($hLTC_4S$)[2] is a 17-kDa integral membrane-bound enzyme that catalyzes the formation of potent smooth muscle-contracting mediators, the cysteinyl leukotrienes, leukotriene (LT) C_4 ((5*S*)-hydroxy-(6*R*)-*S*-glutathionyl-7,9-*trans*-11,14-*cis*-eicosatetraenoic acid) and its metabolites LTD_4 ((5*S*)-hydroxy-(6*R*)-*S*-cysteinylglycyl-7,9-*trans*-11,14-*cis*-eicosatetraenoic acid) and LTE_4 ((5*S*)-hydroxy-(6*R*)-*S*-cysteinyl-7,9-*trans*-11,14-*cis*-eicosatetraenoic acid). The cysteinyl leukotrienes elicit their effects through binding to the cysteinyl leukotriene receptors (1, 2), inducing bronchial smooth muscle contraction, permeability changes in the microcirculation, and immune modulatory actions. The role of cysteinyl leukotrienes in bronchial asthma was established by the therapeutic benefits observed after treatment with inhibitors of the biosynthetic pathway or receptor antagonist (reviewed in Refs. 3 and 4). The formation of LTC_4 catalyzed by $hLTC_4S$ is localized to the outer nuclear membrane. The enzyme conjugates the unstable fatty acid epoxide LTA_4 ((5*S*)-*trans*-5,6-oxido-7,9-*trans*-11,14-*cis*-eicosatetraenoic acid) and GSH to form LTC_4 (see Fig. 1, *left*). $hLTC_4S$ is expressed mainly in leukocytes, and targeted disruption of $hLTC_4S$ in mouse showed reduced antigen-induced inflammation in lung cells (5, 6).

LTC_4S is a member of the MAPEG (membrane-associated proteins in eicosanoid and glutathione metabolism) superfamily of integral membrane proteins (7). This family has six human members and includes three proteins involved in detoxification (MGST1 (microsomal GSH *S*-transferase 1), MGST2, and MGST3) and three proteins with pivotal functions in specific biosynthetic pathways of arachidonic acid metabolism, *viz*. FLAP (five-lipoxygenase-activating protein), LTC_4S, and mPGES-1 (microsomal prostaglandin E synthase 1) (8–12). Probably all MAPEG members, except FLAP, which appears to lack enzymatic function, use a similar mechanism to conjugate glutathione to the lipophilic substrates. Structurally, all but MGST2 and MGST3 have been studied, and mechanistically, MGST1 has been subjected to thorough studies with regard to both substrate preferences and catalytic mechanism (13–15). MGST1 is involved in detoxication of xenobiotic substances by conjugation of GSH to electrophilic compounds (15). MGST2 and MGST3 are thought to have similar catalytic properties as MGST1, although MGST2 has also been shown to be able to produce LTC_4 (8, 11), but have not yet been assigned any specific function. mPGES-1 catalyzes the oxidoreduction of prostaglandin H_2 into prostaglandin E_2 and displays low glutathione transferase and glutathione-dependent peroxidase activities (16). $hLTC_4S$ is highly substrate-specific compared with the other MAPEG family members or GSH transferases, as it accepts only LTA_4, LTA_4

* This work was supported by Swedish Research Council Grants 10350, 80429191, and 20854 and Linneus Grant CERIC, the CIDaT, European Commission Projects FP6 and FP7 (Grants 005033 and 201668), Söderbergs Foundation, a Vinnova SAMPOST position (to D. N.), and a Distinguished Professor Award from the Karolinska Institutet (to J. Z. H.).

⌘ *Author's Choice*—Final version full access.

The atomic coordinates and structure factors (code 3LEO) have been deposited in the Protein Data Bank, Research Collaboratory for Structural Bioinformatics, Rutgers University, New Brunswick, NJ (http://www.rcsb.org/).

[1] To whom correspondence should be addressed. Tel.: 46-8-5248-7612; Fax: 46-8-736-0439; E-mail: jesper.haeggstrom@ki.se.

[2] The abbreviations used are: $hLTC_4S$, human leukotriene C_4 synthase; LT, leukotriene.

methyl ester, and, to a small extent, analog leukotriene epoxides (17, 18).

We previously solved the crystal structure of $hLTC_4S$, revealing a trimeric membrane protein (19). In this study, we wanted to investigate the contribution to catalysis of individual residues at the active site of $hLTC_4S$, and in particular, we wanted to understand the role of Arg-104 during catalysis. Arg-104 has been suggested to activate the GSH cysteine thiol (19, 20) prior to GSH conjugation.

From the crystal structure solved to 2.2 Å (19), the active site of $hLTC_4S$ is well defined with regard to GSH binding. GSH is coordinated to eight residues from two subunits of the trimer (see Fig. 1, *right*), several of which are conserved among members of the MAPEG family (21). The guanidinium group of Arg-104 interacts with the –SH group of GSH at a distance of 3.2 Å, and Arg-104 was therefore suggested to be involved in lowering the pK_a of the thiol proton (19).

In this study, we used site-directed mutagenesis, UV spectroscopy, and x-ray crystallography to investigate the catalytic roles of active-site residues Arg-31, Arg-51, Tyr-59, and Arg-104 in $hLTC_4S$. In particular, we show that Arg-104, but not Arg-31, plays a key role in the enzyme mechanism by activating the GSH thiol and stabilizing the resultant thiolate anion.

EXPERIMENTAL PROCEDURES

Materials—Imidazole, Tris base, NaCl, KCl, Triton X-100, sodium deoxycholate, *S*-hexylglutathione-agarose, probenecid, GSH, and 2-mercaptoethanol were obtained from Sigma. Platinum *Pfx* DNA polymerase and deoxyribonucleotides were from Invitrogen. Dodecyl maltoside was obtained from Anatrace. LTA_4 methyl ester (BIOMOL) in tetrahydrofuran was saponified with 1 M LiOH (6%, v/v) for 48 h at 4 °C. All other chemicals were obtained from common commercial sources.

Site-directed Mutagenesis—The $hLTC_4S$ cDNA (I.M.A.G.E. cDNA clone 5277851, Medical Research Council Geneservice, Cambridge, United Kingdom) was subcloned into pPICZA (Invitrogen). Both the cDNA, supplemented with an N-terminal sequence encoding a His_6 tag, and the vector were PCR-amplified, and the products were co-transformed into $CaCl_2$-competent *Escherichia coli* (TOP10, Invitrogen), utilizing the endogenous recombinase activity of *E. coli* to recombine the fragments. Site-directed mutagenesis was carried out according to the QuikChange protocol (Stratagene, La Jolla, CA). The primers were as follows: 5′-ccgcgcagctcagtctggcaccgctg-3′ and 5′-cagcggtgccagactgagctgcgcgg-3′ for R104S; 5′-ccgcgcagctcgcgctggcaccgctg-3′ and 5′-cagcggtgccagcgcgagctgcgcgg-3′ for R104A; 5′-ccgcgcagctcacgctggcaccgctg-3′ and 5′-cagcggtgccagcgtgagctgcgcgg-3′ for R104T; 5′-ccgcgcagctcaagctggcaccgctg-3′ and 5′-cagcggtgccagcttgagctgcgcgg-3′ for R104K; 5′-atctcggcgcgccaggccttccgcgtg-3′ and 5′-cacgcggaaggcctggcgcgccgagat-3′ for R31Q; 5′-atctcggcgcgcgcggccttccgcgtg-3′ and 5′-cacgcggaaggccgcgcgcgccgagat-3′ for R31A; 5′-gagcgcgtctacgcagcccaggtgaactgc-3′ and 5′-gcagttcacctgggctgcgtagacgcgctc-3 for R51A; 5′-gagcgcgtctaccaagcccaggtgaactgc-3′ and 5′-gcagttcacctgggcttggtagacgcgctc-3 for R51Q; and 5′-aactgcagcgagttcttcccgctgttc-3′ and 5′-gaacagcgggaagaactcgctgcagtt-3′ for Y59F. The mutations and the integrity of the protein-coding part were verified by DNA sequencing (SEQLAB, Göttingen, Germany).

Protein Expression and Purification—The expression vector was transformed into *Pichia pastoris* KM71H cells using the Pichia EasyComp transformation kit (Invitrogen). Recombinant cells were cultivated in baffled flasks in 2.5 liters of buffered minimal yeast medium with glycerol (Invitrogen formula) at 27 °C. When A_{600} reached 8–10, the cells were resuspended in 0.75 liters of buffered minimal yeast medium supplemented every 24 h with 0.6% methanol, and the pH of the medium was adjusted to pH 6–6.5 using 8% NH_3. The cells were harvested after 48 h by centrifugation (2500 × *g*, 6 min) and resuspended in 50 mM Tris-HCl (pH 7.8), 100 mM KCl, and 10% glycerol. The cells were homogenized with glass beads (0.5 mm) using a BeadBeater (BioSpec Products) operated 7 × 1 min on ice. The slurry was filtered through nylon net filters (180 μm; Millipore) and centrifuged (1500 × *g*, 10 min). Membrane-bound proteins in the supernatant were solubilized with Triton X-100 (1%, v/v) and sodium deoxycholate (0.5%, w/v) for 1 h with stirring on ice. After centrifugation (10,000 × *g*, 10 min), the supernatant was supplemented with 10 mM imidazole and loaded on nickel-Sepharose Fast Flow (GE Healthcare). The column was washed with 3 column volumes of buffer A (25 mM Tris-HCl (pH 7.8), 10% glycerol, 0.1% Triton X-100, and 5 mM 2-mercaptoethanol) supplemented with 20 mM imidazole and 0.1 M NaCl, followed by an additional wash with buffer A containing 40 mM imidazole and 0.5 M NaCl. $hLTC_4S$ was eluted with 300 mM imidazole, 0.5 M NaCl, and 0.1 mM GSH in buffer A. The final step of purification was performed on a column packed with *S*-hexylglutathione-agarose. The column was washed with buffer A supplemented with 0.5 M NaCl and 0.1 mM GSH. Pure $hLTC_4S$ was eluted with 25 mM Tris-HCl (pH 7.8), 0.1% Triton X-100, 30 mM probenecid, 5 mM 2-mercaptoethanol, and 0.1 mM GSH. The sample was desalted on PD-10 columns (GE Healthcare) and eluted in 25 mM Tris-HCl (pH 7.8), 10% glycerol, 0.05% Triton X-100, 5 mM 2-mercaptoethanol, and 0.1 mM GSH. After a 5-fold concentration on an Amicon Ultra-15 centrifugal filter device (Millipore), the purified protein was stored frozen at −20 °C.

The enzyme used for spectroscopic studies was, after the immobilized metal ion affinity chromatography step, purified in buffers containing 0.03% (w/v) dodecyl maltoside and in the absence of GSH. As a final step for crystallization purposes, the sample was subjected to a buffer exchange on Superdex 200 16/60 (GE Healthcare) equilibrated with 25 mM Tris-HCl (pH 7.2), 0.03% (w/v) dodecyl maltoside, and 300 mM NaCl. Fractions containing R31Q $hLTC_4S$ were concentrated to 1–3 mg/ml by ultrafiltration. Protein concentrations were determined according to the method of Lowry (Sigma) with BSA as a standard. SDS-PAGE was performed on a PhastSystem (GE Healthcare) utilizing 10–15% gradient gels. Protein bands were visualized with Coomassie Brilliant Blue.

Activity Measurements—To determine the enzyme activity, aliquots of enzyme (0.2 μg for wild-type, R51A, R51Q, Y59F, and R31Q $hLTC_4S$ and 0.3–10 μg for R104A, R104T, R104K, R104S and R31A $hLTC_4S$) were diluted to 100 μl with 25 mM Tris-HCl (pH 7–9.1) supplemented with 0.03% Triton X-100

and 5 mM GSH. The incubations were performed at room temperature with 30 μM LTA_4 and stopped after 15 s by the addition of 200 μl of methanol followed by 100 μl of water. Prostaglandin B_2 (400–500 pmol) was added as an internal standard before reversed phase-HPLC, which was performed on a Waters Nova-Pak C_{18} column (3.9 × 150 mm) eluted with a mixture of acetonitrile/methanol/water/acetic acid (30:20:50:0.1, v/v) at an apparent pH 5.6 and at a flow rate of 0.8 ml/min (LKB 2150 pump). Qualitative analysis was performed by comparison with the retention time of synthetic LTC_4 and the UV absorbance of eluted compounds at 280 nm using a Milton Roy SpectroMonitor 3100 detector. The amount of LTC_4 was quantified by calculating the ratio of the peak area compared with the internal standard prostaglandin B_2. The k_{cat} and K_m values were determined from the initial velocity of the hLTC$_4$S-catalyzed reaction measured as a function of substrate (GSH) concentration. The initial velocity data were fitted to the Michaelis-Menten equation using GraphPad Prism. The k_{cat} value was calculated from the V_{max} and enzyme concentration ([*E*]) according to equation $k_{cat} = V_{max}/[E]$ (see Table 2).

Ultraviolet Difference Spectroscopy—UV spectra were recorded on a Philips PU8720 or Cary 400 Bio spectrophotometer at room temperature. Spectra (200–400 nm) were recorded in 1-cm cuvettes with WT, R104A, and R104S hLTC$_4$S (20 μM) in 100 mM Tris-Cl (pH 7.2) with 0.05% dodecyl maltoside in the presence or absence of 0.5 mM GSH. Difference spectra were obtained by subtracting the spectra of enzyme in buffer without GSH and in buffer with 0.5 mM GSH. The formation of a thiolate anion was measured as an increase in absorbance at 239 nm with $\epsilon_{239} = 5000\ M^{-1}\ cm^{-1}$ (22, 23). Each measurement was repeated at least three times using three different protein batches. The same experiment was performed with 1 mM GSO_3^- added to the cuvette with hLTC$_4$S-GS^-, with GSO_3^- acting as a competitive inhibitor.

Crystallization of R31Q hLTC$_4$S—Crystals of R31Q hLTC$_4$S were grown and cryo-cooled as described (19). Diffraction data were collected to a resolution of 2.1 Å for the complex at beamline ID14-1 at the European Synchrotron Radiation Facility using an ADSC Quantum Q210 detector. Each frame was exposed for 1 s with an oscillation range of 0.5°. The XDS package (24) was used for indexing and integration. Scaling of the data was done using SCALA in the CCP4 suite (25). Native hLTC$_4$S (Protein Data Bank code 2uuh) without ligands or water molecules was used for initial rigid body refinement of the R31Q hLTC$_4$S data. The $F_o - F_c$ maps produced showed clear electron density around position 31 corresponding to the mutation of Arg to Gln. Electron density corresponding to a GSH molecule was also seen in the active site. REFMAC5 (26) in the CCP4i package was used for refinement of coordinates and *B*-factors. COOT (27) was used for molecular modeling.

Structure Solution and Refinement—The refinement of the R31Q hLTC$_4$S structure converged at R_{cryst} and R_{free} of 18 and 20%, respectively. The quality of the final structure was verified using PROCHECK (28). The Ramachandran plot for the R31Q hLTC$_4$S structure showed that 97% of residues were in the most favorable regions and 2% were in the allowed region. The coordinates and structure factors for R31Q hLTC$_4$S have been deposited in the Protein Data Bank (code 3LEO). All figures were made using PyMOL (DeLano Scientific).

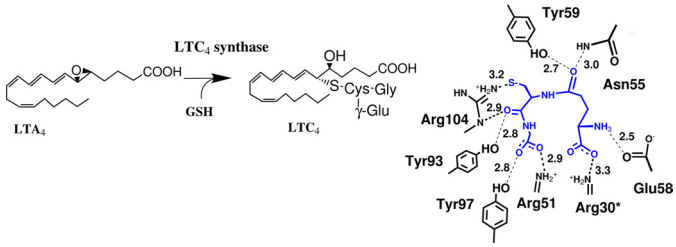

FIGURE 1. *Left*, schematic drawing of the catalytic reaction of hLTC$_4$S. The allylic epoxide LTA_4 is conjugated with GSH at C6 to form LTC_4. *Right*, schematic drawing of how GSH interacts with residues at the active site of hLTC$_4$S. Distances shown are measured in angstroms (from the crystal structure Protein Data Bank code 2uuh). The *asterisk* indicates a residue positioned on the adjacent monomer.

RESULTS AND DISCUSSION

We have studied the contribution of candidate catalytic residues at the active site of hLTC$_4$S to the enzyme's ability to conjugate GSH with LTA_4. The two mechanistically oriented questions we wanted to answer were the possible role of Arg-104 in stabilizing the GSH thiolate anion and the possible role of Arg-31 during epoxide opening. The two residues were mutated, and steady-state kinetics was used to determine the catalytic behavior. UV difference spectroscopy was employed to analyze thiolate anion stabilization by Arg-104, and crystallography was used to study the structure of an Arg-31 mutant. In addition, we mutated and studied the functional roles of Arg-51 and Tyr-59 coordinating GSH at the active site of hLTC$_4$S.

Structural Evidence for the Involvement of Arg-104 in Catalysis—The first suggestions that Arg-104 might be involved in activating the thiol during catalysis of hLTC$_4$S arose when the structure was solved in 2007 (19, 20). The putative active site in the two crystal structures showed a bound GSH with the –SH group in close proximity to the guanidinium group of Arg-104 with a coordination distance of 3.2 Å (Fig. 1, *right*). Examining distances from other residues to the –SH group shows that there is no other good candidate that could activate the thiol.

Mutants of Arg-104—To determine the role of Arg-104 in the formation of the thiolate anion during the hLTC$_4$ conjugation reaction, we mutated Arg-104 to Ala, Ser, Thr, and Lys in separate constructs. The plasmids were transformed into *P. pastoris* cells, and the proteins were expressed and purified using nickel-agarose and *S*-hexylglutathione affinity column chromatography. The ability of the enzymes to bind GSH appeared not to be impaired because they could still be purified using one step of *S*-hexylglutathione affinity chromatography.

Effects of Mutations on Enzyme Activity—All of the Arg-104 mutations strongly reduced the ability of hLTC$_4$S to form LTC_4 as measured by HPLC. The amount of LTC_4 generated by R104A, R104S, R104T, and R104K was so low that, to achieve quantitative data, the amount of protein used in the incubations was increased from 0.2 μg for the WT enzyme to 0.5, 0.6, 6, and 10 μg for the mutants, respectively. Under

TABLE 1

Specific activity of wild-type and mutant $hLTC_4S$ with 5 mM GSH (pH 7.8) and 30 μM LTA_4

Incubations were performed at room temperature for 15 s.

Enzyme	Specific activity	% of WT
	μmol/min mg	
WT	35 ± 0.5	100
R104A	2.0 ± 0.2	5.7
R104S	1.6 ± 0.3	4.6
R104K	0.044 ± 0.02	0.1
R104T	0.4 ± 0.1	1.1
R31Q	10.5 ± 5.9[a]	30
R31A	4.3 ± 0.2	12
R51A	20 ± 5	57
R51Q	10 ± 2	29

[a] Mean value measured from three separate batches.

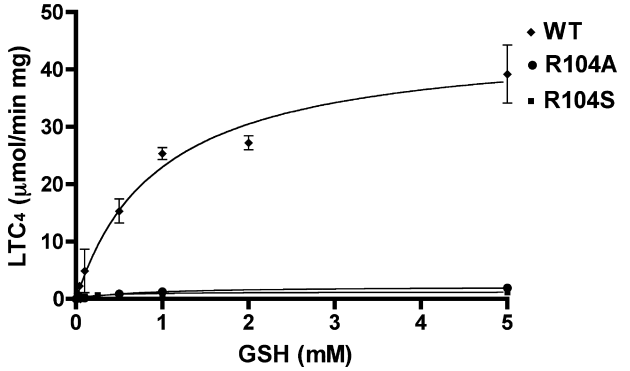

FIGURE 2. **Steady-state kinetic analysis of WT $hLTC_4S$ and Arg-104 mutants.** Shown is the specific activity of WT (0.2 μg), R104A (0.5 μg), and R104S (0.6 μg) $hLTC_4$, where LTA_4 was kept constant at 30 μM and GSH was varied between 0.01 and 5 mM.

these experimental conditions, the percent of the specific activities of the different batches of R104A, R104S, R104T, and R104K compared with the WT enzyme were 5.7, 4.5, 1. and 0.1%, respectively (Table 1). The mutant proteins were subjected to extensive crystallization efforts, in particular, R104A and R104S $hLTC_4S$. Although the proteins yielded crystals, they diffracted to only ~8–10 Å and thus did not allow structural analysis. However, rescue of the enzyme activity of the mutants by increased pH and their ability to bind the affinity column strongly indicate that the mutations had not introduced any significant conformational changes at the active sites (see below).

The small residual activity of R104A and R104S, in which the side chains are considerably shorter, may be explained by increased space for water molecules that can aid in hydroxyl anion-assisted thiolate formation, in line with our experimental observations (see Fig. 3*b*). In the Lys mutant, which has a markedly lower activity, there is little (if any) room for water, and the different structure of the side chain is likely to change the position of the positive charge. In summary, 94.3–99.9% of the activity observed for the wild-type enzyme could be abolished by a single point mutation of Arg-104.

Steady-state kinetics of the R104A and R104S mutants at saturating concentrations of LTA_4 (30 μM) showed a decreased V_{max} but a relatively similar K_m for GSH (Fig. 2 and Table 2). The retained K_m for GSH is in agreement with results obtained from the purification procedure (*i.e.* the mutants bound to an *S*-hexylglutathione affinity column).

TABLE 2

Steady-state kinetic parameters of $hLTC_4S$ obtained at 20 °C and pH 7.8 during incubation for 15 s

In the respective measurements, 0.2 μg of WT, 0.5 μg of R104A, 0.6 μg of R104S, 0.4 μg of R31Q, and 1 μg of R31A $hLTC_4S$ were used.

Enzyme	K_m	V_{max}	k_{cat}	k_{cat}/K_m
	mM	*μmol/min mg*	s^{-1}	$mM^{-1}\ s^{-1}$
WT	0.3 ± 0.06	35 ± 2	11.7	39
R104A	0.5 ± 0.13	2 ± 0.2	0.66	1.3
R104S	0.1 ± 0.09	1.6 ± 0.3	0.5	5
R31Q	0.07 ± 0.07	5.5 ± 0.1	1.8	26
R31A	0.05 ± 0.01	4.3 ± 0.2	1.4	28

Ionization of GSH Bound to $hLTC_4S$—To detect the presence of the thiolate anion, analyses of UV difference spectra were performed. UV difference spectra of GSH bound to WT $hLTC_4S$ were obtained by mixing 0.5 mM GSH with 20 μM $hLTC_4S$ (0.35 mg/ml). Prior to mixing enzyme and GSH, the spectral contributions of free enzyme and free GSH were subtracted. The presence of thiolate was detected from the peak absorbance at 239 nm seen in the spectra from 200 to 300 nm ($\epsilon_{thiolate} = 5000\ M^{-1}\ cm^{-1}$). The experiment was repeated three times with three different batches of enzyme, all yielding the same results. For simplicity, only one representative measurement is shown in Fig. 3*a*. The concentration of thiolate anion formed was calculated to be 17.3 ± 4.2 μM (mean ± S.D., $n = 3$) using the WT enzyme, which thus equaled the concentration of enzyme used in the experiment (20 μM), suggesting a 1:1 stoichiometry in the binding of thiolate to the enzyme (one thiolate/subunit). The same stoichiometry was obtained in pre-steady-state kinetics experiments measuring the rate of thiolate anion formation in $hLTC_4S$.[3] It appears that $hLTC_4S$ harbors three catalytically competent active sites/homotrimer, in contrast to MGST1, which displays one-third of the active sites reactive (29).

Analyses of UV difference spectra for R104A and R104S $hLTC_4S$ failed to produce a visible thiolate at 239 nm, further corroborating the notion that Arg-104 is important for GSH activation. To ascertain that the peak observed at 239 nm for WT $hLTC_4S$ was due to GS^- formation at the active site, we used a competitive inhibitor to GSH, *viz.* GSO_3^-. This compound was incubated with WT $hLTC_4S$ prior to mixing the enzyme with GSH, which completely prevented the appearance of a thiolate signal (Fig. 3*a*). Hence, a functional sulfhydryl group is needed, as well as a guanidinium group from Arg-104, to achieve a thiolate signal.

pH Dependence of LTC_4 Production—The formation of the thiolate anion is considered a key step in GST catalysis (30). Because the sulfhydryl group of GSH is a weak acid with a pK_a of 9 (23, 31), thiolate anions form spontaneously only at high pH. Accordingly, it should be possible to rescue some GSH-conjugating capacity from inactive mutants at higher pH if the bound GSH can form a thiolate by the influence of solvent pH. As depicted in Fig. 3*b*, the activity of the WT enzyme was not significantly increased when the pH was increased from 7.0 to 9.1. This suggests that the catalytic machinery had already reduced the activation energy of the conjugation reac-

[3] A. Rinaldo-Matthis, J. Holm, A. Wetterholm, R. Morgenstern, and J. Z. Haeggström, unpublished data.

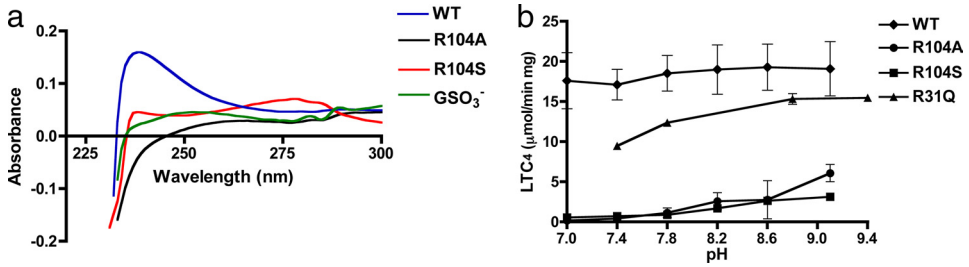

FIGURE 3. *a*, UV difference spectra of $hLTC_4S$. The *blue trace* shows the WT enzyme mixed with 0.5 mM GSH. The *black trace* corresponds to R104A $hLTC_4S$ mixed with GSH. The *red trace* corresponds to R104S $hLTC_4S$ mixed with GSH. The *green trace* is the WT enzyme mixed with 1 mM GSH and GSO_3^-. A UV scan from 200 to 400 nm shows that a thiolate anion gives rise to a peak at 239 nm in the spectrum of $hLTC_4S$ but not in spectra from the mutant and WT enzymes incubated with the competitive inhibitor (GSO_3^-). *b*, the specific activity of $hLTC_4S$ is compared with those of R104A, R104S, and R31Q $hLTC_4S$ when the pH was changed between 7 and 9. The WT enzyme did not show pH dependence to the same extent as the R104A and R104S mutants. The non-enzymatic formation of LTC_4 did not reach detectable levels at any pH in buffer controls without enzyme.

tion so efficiently that an increase in pH did not make a significant difference. In contrast, for R104S and R104A, a 30–40-fold increase in activity was observed over the same pH range. Calculated as a percent of the wild-type activity, R104A increased its ability to generate LTC_4 from 0.9% at pH 7.0 to 32% at pH 9.1, demonstrating that alkaline conditions can partially compensate for the loss of Arg-104. Of note, the fact that enzyme activity in R104A and R104S $hLTC_4S$ could be rescued demonstrates that the amino acid substitutions have not caused any significant alterations of the protein conformations.

Mutations of Arg-31—During the catalytic reaction of $hLTC_4S$, the thiolate formed at the active site is thought to attack C6 of the oxirane ring of LTA_4 concomitant with the opening of the LTA_4 epoxide, leading to formation of a hydroxyl group at C5. It is reasonable to anticipate that a residue might participate in epoxide opening by stabilizing the developing negative oxyanion. From the crystal structures of $hLTC_4S$, Arg-31 was suggested to serve this role (10, 11). Thus, it was speculated that Arg-31 would move closer to the epoxide of LTA_4 during catalysis and stabilize the negatively charged epoxide oxygen prior to the attack of the thiolate anion. However, in the crystal structures, Arg-31 is disordered and partially lacks electron density in the structures, making it difficult to determine its exact position and potential role in catalysis. To probe the function of Arg-31, we exchanged this residue with Ala or Gln. The R31Q and R31A mutants retained 30 and 12%, respectively, of the activity of WT $hLTC_4S$ (see Table 1), suggesting that this residue does not have a crucial role during catalysis. Rather, the mutation of Arg-31 may introduce some smaller structural changes in the active-site region that influence binding of substrates. To further analyze the role of Arg-31, we solved the crystal structure of R31Q $hLTC_4S$ in complex with GSH to 2.1 Å resolution (Table 3). The structure showed Arg-31 substituted with a defined electron density representing Gln-31 pointing away from the active site with a distance between its functional group and the GSH thiol of 7 Å (Fig. 4). To date, there is no structural evidence defining the exact position of the epoxide during catalysis because a structure of a product (LTC_4) complex and/or substrate (LTA_4) complex is missing. Pending more detailed structural and kinetic information on substrate binding, our data do not favor any specific role for Arg-31 in enzyme catalysis.

TABLE 3

Data processing and refinement statistics of R31Q $hLTC_4S$ in complex with GSH

r.m.s., root mean square; PDB, Protein Data Bank.

Wavelength (Å)	0.93340
Space group	F23
Cell dimensions	
$a = b = c$ (Å)	170
$\alpha = \beta = \gamma$	90°
Resolution (Å)	2.1
Unique reflections	31,117
All reflections	221,628
Completeness (%)[a]	99.1 (100)
Multiplicity[a]	7.1 (7.5)
R_{sym} (%)[a,b]	13.4 (40.6)
I/σ^a	20.8 (4.1)
No. of protein atoms	1189
No. of waters	61
No. of ligands	12
R-factor	18
R_{free}	20.4
Average *B*-factor	35
r.m.s. bond (Å)	0.018
r.m.s. angle	1.77°
Ramachandran analysis	
Most favored regions	97.3
Allowed regions	2.0
Disallowed regions	0.7
PDB code	3LEO

[a] Values for the highest resolution shell are given in parentheses.
[b] $R_{sym} = (\Sigma_{hkl}\Sigma_i|I_{i(hlk)} - \langle I_{(hkl)}\rangle|)/\Sigma_{hkl}\Sigma_i I_{i(hkl)}$ for n independent reflections and observations of a given reflection, $\langle I_{(hkl)}\rangle$ is the average intensity of the i observation.

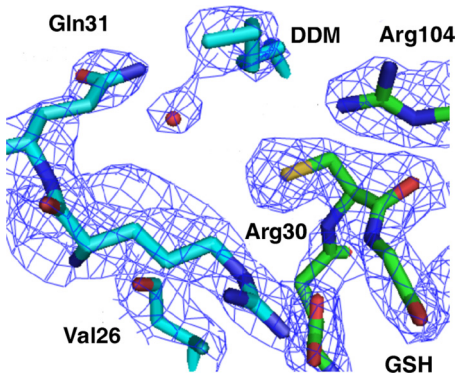

FIGURE 4. **Active site of the R31Q $hLTC_4S$ structure where a $2F_o - F_c$ map electron density is contoured at 1σ.** The protein is shown in *cyan*, and GSH in shown in *green*. *DDM*, dodecyl maltoside.

Other Interactions with GSH—Previous mutagenesis studies of Arg-51, with activity measurements in microsomal membranes, indicated that this residue has a crucial role in LTC_4 production (32). The data presented here on purified proteins

of mutants R51A and R51Q show a retained activity of 30–60% compared with the WT enzyme (Table 1), which suggests that Arg-51 is not essential for catalysis. In the crystal structure of $hLTC_4S$ in complex with GSH, Arg-51 is coordinating one of the carboxyl groups of GSH with a distance of 2.9 Å in concert with Tyr-97 (Fig. 1, *right*). In agreement with previous results, Tyr-59 does not seem to be essential for catalysis because 90% of the activity is retained in Y59F $hLTC_4S$ compared with the WT enzyme (data not shown). It is interesting to note that mutations of Tyr-59 and Arg-51, both of which are involved in GSH binding, have only small catalytic effects, suggesting that the GSH-binding mode is maintained in these mutations.

A Catalytic Arg Residue, a Common Theme among Microsomal GSTs—The enzymatic ability to lower the pK_a of the sulfhydryl group of GSH is central for GSH-conjugating enzymes such as $hLTC_4S$. The thiol of GSH has a pK_a of 9 in aqueous solution (23, 31), and several GSH-conjugating enzymes have been shown to reduce the pK_a of the same thiol to ~6–7. In MGST1, a thiolate has been observed (33), and structural as well as catalytic similarities to LTC_4S (34) suggest that an Arg is involved in the formation and stabilization of the critical GS^-. Although mPGES-1 is an endoperoxide isomerase, it is believed to utilize a thiolate, and the three-dimensional structure and the kinetics of a mutant form of this enzyme suggest that an Arg is involved in catalysis (35). Furthermore, comparing the primary structure of $hLTC_4S$ with those of MGST2 and MGST3 shows a conserved Arg in the latter two enzymes that corresponds to Arg-104 in $hLTC_4S$ (21). On the other hand, FLAP, for which no enzyme activity has been identified, lacks a conserved Arg. It therefore seems possible that all catalytically competent MAPEG family members use an Arg to stabilize thiolate formation during catalysis.

In soluble GSH transferases, mutagenetic analyses combined with UV difference spectra have shown that Tyr or Ser is the most common residue involved in activating thiolate anions, and it has been reported that Arg can also be important in the mechanism (30, 36, 37). However, a critical role of a single Arg, as in $hLTC_4S$, appears unique, and further work will show whether it represents a structure-function paradigm common to all microsomal GSH transferases.

REFERENCES

1. Lynch, K. R., O'Neill, G. P., Liu, Q., Im, D. S., Sawyer, N., Metters, K. M., Coulombe, N., Abramovitz, M., Figueroa, D. J., Zeng, Z., Connolly, B. M., Bai, C., Austin, C. P., Chateauneuf, A., Stocco, R., Greig, G. M., Kargman, S., Hooks, S. B., Hosfield, E., Williams, D. L., Jr., Ford-Hutchinson, A. W., Caskey, C. T., and Evans, J. F. (1999) *Nature* **399,** 789–793
2. Heise, C. E., O'Dowd, B. F., Figueroa, D. J., Sawyer, N., Nguyen, T., Im, D. S., Stocco, R., Bellefeuille, J. N., Abramovitz, M., Cheng, R., Williams, D. L., Jr., Zeng, Z., Liu, Q., Ma, L., Clements, M. K., Coulombe, N., Liu, Y., Austin, C. P., George, S. R., O'Neill, G. P., Metters, K. M., Lynch, K. R., and Evans, J. F. (2000) *J. Biol. Chem.* **275,** 30531–30536
3. Peters-Golden, M., and Henderson, W. R., Jr. (2007) *N. Engl. J. Med.* **357,** 1841–1854
4. Rinaldo-Matthis, A., and Haeggstrom, J. Z. (2010) *Biochimie* **6,** 676–681
5. Beller, T. C., Maekawa, A., Friend, D. S., Austen, K. F., and Kanaoka, Y. (2004) *J. Biol. Chem.* **279,** 46129–46134
6. Kim, D. C., Hsu, F. I., Barrett, N. A., Friend, D. S., Grenningloh, R., Ho, I. C., Al-Garawi, A., Lora, J. M., Lam, B. K., Austen, K. F., and Kanaoka, Y. (2006) *J. Immunol.* **176,** 4440–4448
7. Jakobsson, P. J., Morgenstern, R., Mancini, J., Ford-Hutchinson, A., and Persson, B. (1999) *Protein Sci.* **8,** 689–692
8. Jakobsson, P. J., Mancini, J. A., Riendeau, D., and Ford-Hutchinson, A. W. (1997) *J. Biol. Chem.* **272,** 22934–22939
9. Samuelsson, B. (1983) *Science* **220,** 568–575
10. Ford-Hutchinson, A. W., Gresser, M., and Young, R. N. (1994) *Annu. Rev. Biochem.* **63,** 383–417
11. Jakobsson, P. J., Scoggan, K. A., Yergey, J., Mancini, J. A., and Ford-Hutchinson, A. W. (1997) *J. Lipid Mediat. Cell Signal.* **17,** 15–19
12. Jakobsson, P. J., Thorén, S., Morgenstern, R., and Samuelsson, B. (1999) *Proc. Natl. Acad. Sci. U.S.A.* **96,** 7220–7225
13. Morgenstern, R., and DePierre, J. W. (1983) *Eur. J. Biochem.* **134,** 591–597
14. Svensson, R., Alander, J., Armstrong, R. N., and Morgenstern, R. (2004) *Biochemistry* **43,** 8869–8877
15. Siritantikorn, A., Johansson, K., Ahlen, K., Rinaldi, R., Suthiphongchai, T., Wilairat, P., and Morgenstern, R. (2007) *Biochem. Biophys. Res. Commun.* **355,** 592–596
16. Thorén, S., Weinander, R., Saha, S., Jegerschöld, C., Pettersson, P. L., Samuelsson, B., Hebert, H., Hamberg, M., Morgenstern, R., and Jakobsson, P. J. (2003) *J. Biol. Chem.* **278,** 22199–22209
17. Izumi, T., Honda, Z., Ohishi, N., Kitamura, S., Tsuchida, S., Sato, K., Shimizu, T., and Seyama, Y. (1988) *Biochim. Biophys. Acta* **959,** 305–315
18. Yoshimoto, T., Soberman, R. J., Spur, B., and Austen, K. F. (1988) *J. Clin. Invest.* **81,** 866–871
19. Martinez Molina, D., Wetterholm, A., Kohl, A., McCarthy, A. A., Niegowski, D., Ohlson, E., Hammarberg, T., Eshaghi, S., Haeggström, J. Z., and Nordlund, P. (2007) *Nature* **448,** 613–616
20. Ago, H., Kanaoka, Y., Irikura, D., Lam, B. K., Shimamura, T., Austen, K. F., and Miyano, M. (2007) *Nature* **448,** 609–612
21. Martinez Molina, D., Eshaghi, S., and Nordlund, P. (2008) *Curr. Opin. Struct. Biol.* **18,** 442–449
22. Graminski, G. F., Zhang, P. H., Sesay, M. A., Ammon, H. L., and Armstrong, R. N. (1989) *Biochemistry* **28,** 6252–6258
23. Graminski, G. F., Kubo, Y., and Armstrong, R. N. (1989) *Biochemistry* **28,** 3562–3568
24. Kabsch, W. (1988) *J. Appl. Crystallogr.* **21,** 67–72
25. Potterton, E., Briggs, P., Turkenburg, M., and Dodson, E. (2003) *Acta Crystallogr. D Biol. Crystallogr.* **59,** 1131–1137
26. Murshudov, G. N., Vagin, A. A., and Dodson, E. J. (1997) *Acta Crystallogr. D Biol. Crystallogr.* **53,** 240–255
27. Emsley, P., and Cowtan, K. (2004) *Acta Crystallogr. D Biol. Crystallogr.* **60,** 2126–2132
28. Laskowski, R. A., MacArthur, M. W., Moss, D. S., and Thornton, J. M. (1993) *J. Appl. Crystallogr.* **26,** 283–291
29. Alander, J., Lengqvist, J., Holm, P. J., Svensson, R., Gerbaux, P., Heuvel, R. H., Hebert, H., Griffiths, W. J., Armstrong, R. N., and Morgenstern, R. (2009) *Arch. Biochem. Biophys.* **487,** 42–48
30. Armstrong, R. N. (1997) *Chem. Res. Toxicol.* **10,** 2–18
31. Chen, W. J., Graminski, G. F., and Armstrong, R. N. (1988) *Biochemistry* **27,** 647–654
32. Lam, B. K., Penrose, J. F., Xu, K., Baldasaro, M. H., and Austen, K. F. (1997) *J. Biol. Chem.* **272,** 13923–13928
33. Morgenstern, R., Svensson, R., Bernat, B. A., and Armstrong, R. N. (2001) *Biochemistry* **40,** 3378–3384
34. Holm, P. J., Bhakat, P., Jegerschöld, C., Gyobu, N., Mitsuoka, K., Fujiyoshi, Y., Morgenstern, R., and Hebert, H. (2006) *J. Mol. Biol.* **360,** 934–945
35. Hammarberg, T., Hamberg, M., Wetterholm, A., Hansson, H., Samuelsson, B., and Haeggström, J. Z. (2009) *J. Biol. Chem.* **284,** 301–305
36. Caccuri, A. M., Antonini, G., Board, P. G., Flanagan, J., Parker, M. W., Paolesse, R., Turella, P., Federici, G., Lo Bello, M., and Ricci, G. (2001) *J. Biol. Chem.* **276,** 5427–5431
37. Patskovsky, Y. V., Patskovska, L. N., and Listowsky, I. (2000) *J. Biol. Chem.* **275,** 3296–3304